Nanoscale

Cite this: *Nanoscale*, 2012, **4**, 4450

www.rsc.org/nanoscale

COMMUNICATION

Highly controlled synthesis of nanometric gold particles by citrate reduction using the short mixing, heating and quenching times achievable in a microfluidic device†

Jamal Ftouni,[abd] Maël Penhoat,*[bd] Ahmed Addad,[cd] Edmond Payen,[ad] Christian Rolando[bd] and Jean-Sébastien Girardon*[ad]

Received 5th November 2011, Accepted 28th April 2012
DOI: 10.1039/c2nr11666a

Homodispersed 1.8 nm gold nanoparticles were obtained reproducibly in high yields using the classical Turkevich protocol at a high concentration in a continuous flow capillary reactor. The microfluidic reactor made from commercially available items permitted short mixing, heating and quenching times which are the key parameters of this synthesis.

For decades, chemically synthesized nanoparticles have been key elements in catalysis,[1a,b] optics[1c,d] and biological assays.[1e,f] Several procedures have been described in the literature for the synthesis of gold nanoparticles which have been known since antiquity. The first modern protocol was developed and studied by Turkevich and co-workers more than fifty years ago.[2] This protocol is based on the reduction of $HAuCl_4$ by sodium citrate in boiling water and affords particles with a 15 nm average size under classical conditions.[3] Sodium citrate plays a dual role: (i) it reduces the gold precursor and (ii) it stabilizes the gold nanoparticles by coating the surface thus preventing the agglomeration process.[2a] Other procedures have been developed later in order to decrease the particle diameter by changing the reducing agent and by adding stabilizing agents such as organic molecules or polymers.[4] However, these procedures have led to gold nanoparticles enrobed in stabilizing organic materials which may be less effective as catalysts.

Nanoparticles are generally synthesized in classical vessels (batch mode), which leads to poor size distribution control, especially during scaling-up.[5a] This dispersion is mostly induced by the difficulty to accurately control the reaction temperature during the heating and cooling phases which govern the nucleation and growth processes arising in nanoparticle synthesis.[5b] Nowadays, micro- and nanofluidic technologies are disciplines in rapid development, offering a solution to improve the control of the reaction parameters of nanomaterial synthesis based on a faster heat transfer[5c] and mixing[5d] as a result of the increased surface area-to-volume ratio.[5e,f] The first gold nanoparticle synthesis in a microsystem was reported by Wagner *et al.* who studied the growth of gold nanoparticle seeds in a glass microchannel reactor at room temperature.[6a] The same authors described the synthesis of polyvinyl alcohol (PVA) stabilized gold or gold–silver nanoparticles by sodium borohydride reduction, also at room temperature.[6b] Under similar conditions, Tsukuda *et al.* prepared 1.3 nm size poly(*N*-vinyl-2-pyrrolidone) (PVP) stabilized gold particles using a micromixer at a high flow rate (30 mL min^{-1}). These particles exhibited good catalytic properties for the oxidation of para-hydroxybenzyl alcohol by molecular oxygen.[6c] More recently, Yang *et al.* developed an integrated microsystem including pneumatic pumps and a mixing chamber in polydimethylsiloxane (PDMS) which has been applied to the synthesis of gold nanoparticles using Turkevich's protocol. By changing the ratio of the reactants (gold(III) and citrate solutions), particles with sizes ranging from 19 to 58 nm were obtained.[6d] A microfluidic setup was also used for studying *in situ* gold nanoparticle formation by SAXS and XANES spectroscopies.[6e]

In the present study, we describe the transposition of Turkevich's classic gold nanoparticle synthesis under continuous flow conditions

[a]*Unité de Catalyse et de Chimie du Solide (UMR CNRS 8181), Université Lille 1-Sciences et Technologies, 59655 Villeneuve d'Ascq Cedex, France. E-mail: jean-sebastien.girardon@univ-lille1.fr*
[b]*Miniaturisation pour la Synthèse, l'Analyse et la Proteomique (USR CNRS 3290), Université Lille 1 - Sciences et Technologies, 59655 Villeneuve d'Ascq, France. E-mail: mael.penhoat@univ-lille1.fr*
[c]*Unité Matériaux et Transformations (UMR CNRS 8207), Université Lille 1 - Sciences et Technologies, 59655 Villeneuve d'Ascq Cedex, France*
[d]*Institut Michel Eugène Chevreul (FR CNRS 2638), Université Lille 1 - Sciences et Technologies, 59655 Villeneuve d'Ascq, France*
† Electronic supplementary information (ESI) available: Description of the microfluidic device, protocol for gold nanoparticle synthesis in batch and in the microsystem, and gold nanoparticle size distribution raw data. See DOI: 10.1039/c2nr11666a

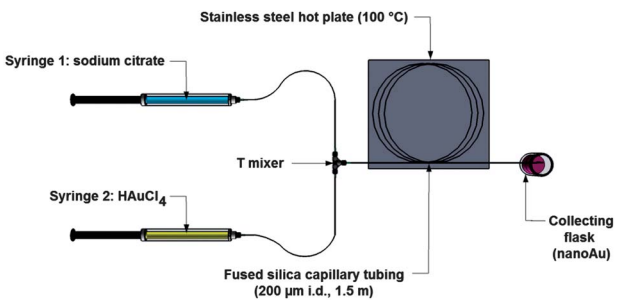

Fig. 1 Microfluidic set-up used for gold nanoparticle synthesis.

using two glass syringes, a syringe pump, a tee mixer to combine the reagents and a 1.5 m × 200 μm i.d. fused silica capillary as a microreactor heated at 100 °C using a heating plate. This set-up, presented in Fig. 1, is based on commercially available devices, which are present in most laboratories.[7] It allows fast heating of the mixed reagents and fast reaction quenching. With this set-up, the fluid sees only inert surfaces made of glass, PEEK® and fused silica, which prevents the reduction of the gold precursor(III) solution by the metallic surfaces. With this set-up, Gastight® glass syringes easily sustain a 150 μL min^{-1} total flow rate (75 μL min^{-1} per syringe) without leaking or breaking, which corresponds to a minimum residence time of 20 seconds in our system.

The critical reaction time of Turkevich's protocol as well as the size of the obtained particles are well known to depend strongly on heating temperature, pH,[8a] gold concentration and gold to reducing agent ratio.[8b] Starting from a 2.94 × 10^{-4} mol L^{-1} $HAuCl_4$ solution, a 0.41 citrate to gold ratio led to a 850 s reaction time and an average particle size of 147 nm at boiling water temperature whereas a 2.58 ratio led to a 145 s reaction time and a 16 nm diameter.[8c] Using higher concentration led to a reduced reduction time and decreasing the reaction temperature below boiling water increased the reduction time by several orders of magnitude.[8d] The pH of the solution also plays a key role because the size decreases from acid to basic pH and reaches a plateau at the pH of a pure sodium citrate solution.[8e] The reaction is also sensitive to the isotopic effect since the use of heavy water as solvent leads to a decrease in the particle size and dispersion.[8f] Recently Ojea-Jiménez *et al.*[9a] and Sivaraman *et al.*[9b] showed the strong influence of the mixing order, as the reverse addition of boiling citrate leads to reduction of nanoparticle size and narrows the size distribution. A fast quenching rate also proves to be critical to get small nanoparticles.[9c] At the opposite, the slow reduction of $HAuCl_4$ in toluene by amines allows to produce micrometric crystals with well defined shapes.[8d] Here we explore a new way for obtaining gold nanoparticles by heating and cooling the reaction mixture at a high rate using a microfluidic continuous flow capillary reactor.

We were delighted that dynamic light scattering (DLS) analysis (Fig. 2) gave an average nanoparticle diameter size around 1.8 nm for a synthesis performed with a concentrated $HAuCl_4$ solution (5.4 × 10^{-3} mol L^{-1}) and a citrate to gold ratio of 3.15 in the microfluidic device with a residence time of 35 s (flow rate 80 μL min^{-1}) at 100 °C (distribution a). Particles made in classical glassware using a concentration of gold precursor divided by ten but with the same 3.15 citrate to gold ratio gave, after 30 minutes, the 15 nm average diameter distribution (b) described in the literature.[3b] However, a batch experiment using the concentrations used in the microfluidic device led to an intractable black slurry. The quality of the mixing of two solutions with different pH (7.60 here for the citrate solution and 2.45 for the gold solution) may also play a role as in the classical Villermaux–Dushman iodine–iodate dismutation reaction used as a mixing efficiency test.[10]

Fig. 3, upper panel, shows the variation of the nanoparticle DLS distribution when the residence time is varied from 35 to 95 s (flow rates ranging from 30 to 80 μL min^{-1}), all the other parameters remaining unchanged. The distribution is much sharper at low residence time and widens after 48 s. In parallel, when the residence time was increased, the diameter started to decrease slightly from 1.8 nm down to 1.5 nm and then increased again up to 3.0 nm after 48 s (Fig. 3, lower panel). The transition which occurs near 48 s reminds of the change in several physical parameters occurring early in the Turkevich protocol when the solution proceeds from the nucleation to the growth step.[11a] The size of 1.8 nm obtained at high flow rate is close to the size of the closed-shell Au_{55} particles, which may explain this stability.[11b]

The two parts of the curve at times lower and higher to the time corresponding to the minimum particle size are due to two very different phenomena. At long time the particle size increases linearly as predicted by the two step Finke–Watzky model.[11c] At short time

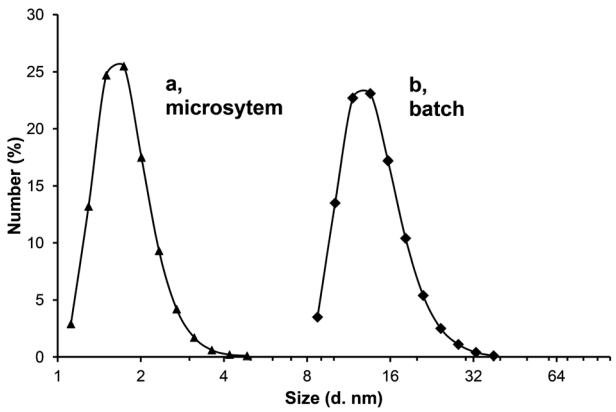

Fig. 2 DLS distribution of gold nanoparticles synthesized in the microfluidic device (a) and in classical glassware (b). Note the logarithmic scale for the size.

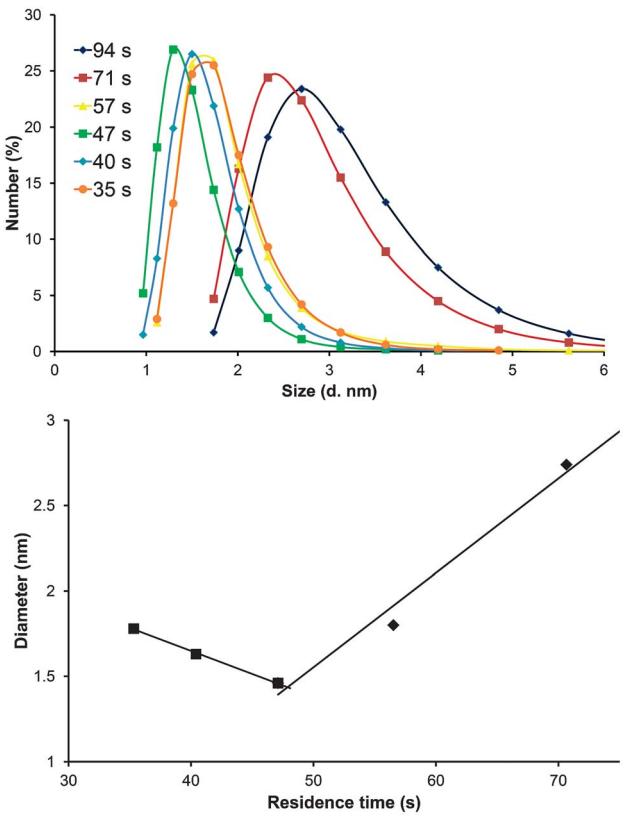

Fig. 3 Upper panel: variation of gold nanoparticle DLS distribution with residence time. Lower panel: variation of gold nanoparticle average diameter with residence time.

not enough nuclei are formed leading to a slightly faster growth of the existing ones. In order to further explore the variation of gold nanoparticle diameter we then studied the effect of sodium citrate to gold precursor ratio at a constant flow rate. The curve shown in Fig. 4 exhibits a sharp minimum for sodium citrate to $HAuCl_4$ ratio of 3.15 close to the 3.5 value given in Frens' protocol. Recently a very similar curve was observed by Ji *et al.* with a minimum diameter obtained with a ratio in the same range.[8e] Here too the two parts of the curve are explained by two different phenomena. At low sodium citrate to $HAuCl_4$ ratio the size increases as there is an excess of gold precursor compared to formed nuclei whereas at high sodium citrate to $HAuCl_4$ ratio the size increased as the stabilization of the nanoparticles is diminished by the increase of negative charges in the solution.

Finally we investigated the effect of temperature on the gold nanoparticle diameter. The particle size was found to be very sensitive to the temperature. In the range 60 to 100 °C the diameter is inversely proportional to the absolute temperature (Fig. 5). This behavior is expected for particles obtained at the onset of nucleation for which the diameter is given according to LaMer theory by the equation:[12]

$$d = \frac{4\gamma V_m}{RT \ln S}$$

where V_m is the molar volume of the gold crystal, γ is the surface energy per unit area and S is the supersaturation (ratio of solution concentration to equilibrium saturation concentration).

The particles obtained at different flow rates (residence time from 35 to 94 s) were also analyzed by UV-visible spectroscopy (Fig. 6, upper panel) immediately after synthesis in the microfluidic system. The spectrum (b) of the classical Turkevich gold nanoparticles exhibits the feature of the metallic gold spherical nanoparticles with the surface plasmon resonance (SPR) band at 520 nm and the charge transfer band above 270 nm.[13a] The absence of the absorption peak at 300 nm characteristic of Au^{3+} (spectrum c) confirms the total reduction of the gold precursor ($HAuCl_4$). In the case of nanoparticles obtained in the microfluidic device (spectrum a), no Au^{3+} species and no surface plasmon resonance (SPR) peak were identified, which suggests the presence of smaller nanoparticles. Indeed it has been shown that gold nanoparticles with a diameter below 3 nm do not exhibit the SPR band.[13b] The absence of a plasmon peak demonstrates that the obtained particles are homogeneous and that

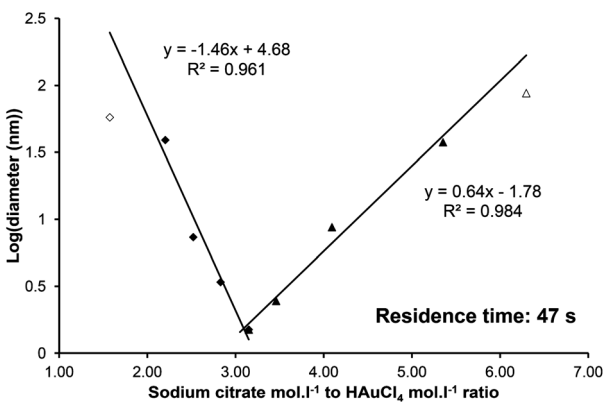

Fig. 4 Variation of gold nanoparticle average diameter logarithm with sodium citrate to $HAuCl_4$ ratio at constant gold concentration and at a fixed residence time of 47 s (flow rate 60 μL min^{-1}).

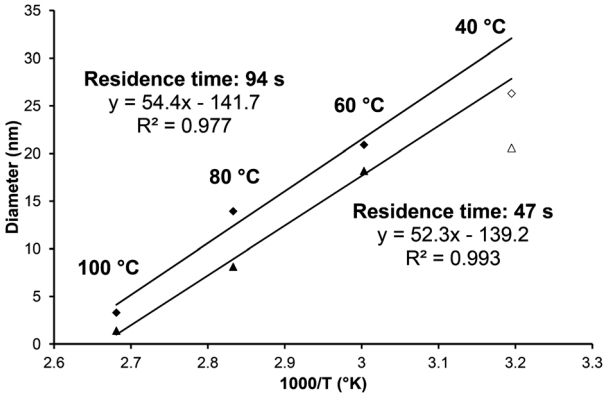

Fig. 5 Variation of gold nanoparticle average diameter with temperature at constant residence times of 47 s and 94 s (flow rate 60 and 30 μL min^{-1} reciprocally).

there are no particles of higher diameter present, since the absorption of the plasmon peak increases sharply with the gold nanoparticle diameter.

In Fig. 6 the middle panel shows the absorbance at long wavelength of the nanoparticles obtained at various flow rates. The absorbance increases linearly with residence time and is well correlated with the mean diameter obtained by DLS (Fig. 6, lower panel). For diameters below 3 nm surface scattering is the most important contribution to the absorbance.[13c] Surface scattering frequency is given by:

$$\omega_s = A\frac{v_F}{R}$$

where v_F is the Fermi velocity, R the radius of the particle and A a constant varying according to models from 0.1 to 2.0. Numerical simulations based on the article by Whetten and collaborators[13c] show that the absorption for small particles exhibits a bell-shaped curve which increases with particle diameter, reaches a maximum and then decreases. The precise position of the maximum depends on the permittivity of the surrounding medium ε_m and on the A parameter. The position decreases both with A and ε_m values and varies from less than 1 nm to 2 nm. This latter value was obtained assuming $A = 2$ and a permittivity $\varepsilon_m = 1.75$ (close to the water value at optical frequencies). This numerical simulation predicts an absorbance proportional to the nanoparticle radius in agreement with data presented in the lower panel of Fig. 6. This behavior has been observed by Duff *et al.* for gold nanoparticles stabilized by tetrakis(hydroxymethyl)-phosphonium chloride.[13d]

As discussed by Khlebtsov *et al.*, the transformation of scattering to size distributions depends strongly on several parameters linked to the aspect ratio which are hidden in commercially available DLS equipment.[14] So, the nanoparticles were further analyzed by transmission electron microscopy (TEM) (Fig. 7) in order to confirm the DLS analysis. No centrifugation or any other kind of filtration was performed before the TEM analysis. The TEM pictures clearly show the nanoparticles with typical diameters around 16.2 ± 2.2 nm for the classical preparation (a), and 2.0 ± 0.5 nm for the particles obtained within the microfluidic device at a flow rate of 60 μL min^{-1} (b). These results are in good agreement with the DLS analysis.

Selected area electron diffraction (SAED) (Fig. 8) was performed inside the TEM to confirm the nature of the observed nanoparticles

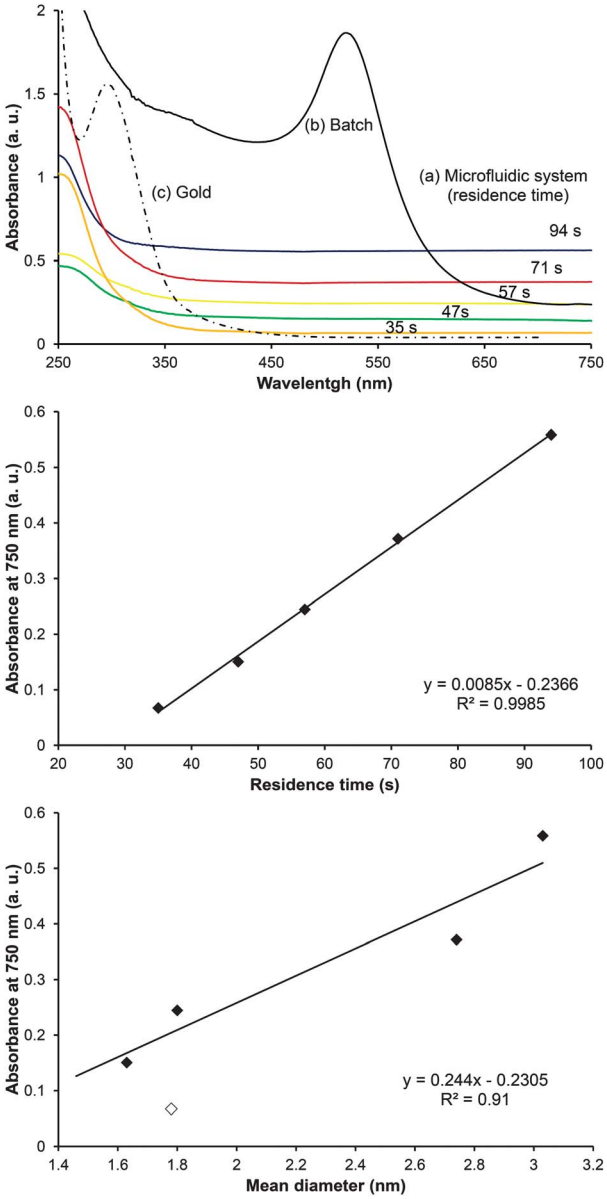

Fig. 6 Upper panel: UV-visible spectra of the gold nanoparticles obtained (a) in the microfluidic device at different residence times, (b) in batch mode, and (c) of the $HAuCl_4$ gold precursor solution; middle panel: variation of the visible absorption at 750 nm with residence time; lower panel: variation of the visible absorption at 750 nm with mean diameter obtained by DLS.

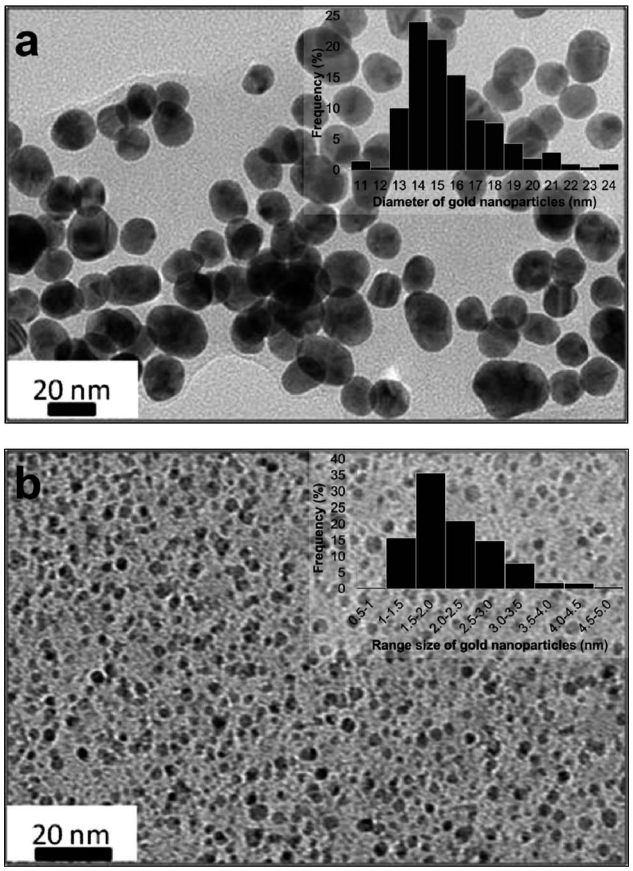

Fig. 7 Transmission electron microscopy (TEM) images and size distribution of gold nanoparticles obtained (a) in the glassware synthesis, upper panel, and (b) in the microfluidic device at a flow rate of 60 μL min^{-1} (residence time 47 s), lower panel.

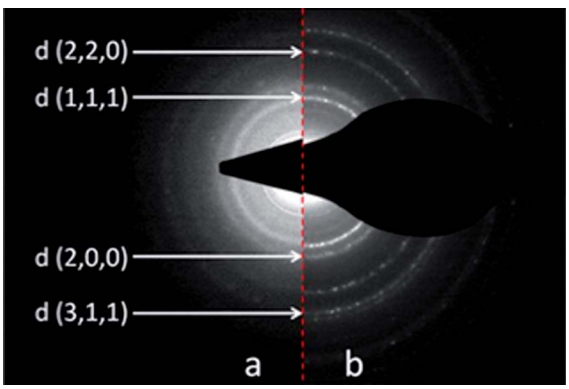

Fig. 8 SAED pattern of the gold nanoparticles obtained *via* batch mode (right) and microfluidic device (left).

and their crystal structure. The observed *d*-spacings at 2.4, 2.1, 1.5 and 1.3 Å correspond respectively to the (111), (200), (220) and (331) Miller indices of fcc (face-centered cubic) gold crystals.[15] The SAED pattern on the left panel (a) is more diffuse due to the smaller diameter of the gold nanoparticles obtained in the microfluidic device, compared to the larger diameter of the gold nanoparticle obtained in batch mode (b), which affords a sharper diffraction pattern.

In conclusion, new gold nanoparticles have been developed with a high control of the synthesis parameters such as reactant mixing, temperature and reaction time control. We describe an original microfluidic set-up which can be easily replicated to produce low diameter gold nanoparticles (average diameter < 2 nm) protected by sodium citrate. Such low size gold nanoparticles have never been obtained with the classical Turkevich process. Furthermore these nanoparticles are weakly stabilized and so they may be useful for testing new ligands by displacement while preserving their size both for physical chemistry experiments and catalysis.

The authors thank the Region Nord-Pas de Calais and the CNRS for a PhD grant to JF, and the Institut Michel E. Chevreul (FR CNRS 2638) for a Young Investigator Grant funded by the "Contrat

de Projet État-Région" (CPER) to JSG and MP. The authors thank Pr Didier Tanré for helpful insight into Mie theory and Dr Maria van Agthoven for her help with editing this manuscript.

Notes and references

1 (*a*) M. B. Cortie and E. van der Lingen, *Mater. Forum*, 2002, **26**, 1; (*b*) M. Haruta and M. Date, *Appl. Catal., A*, 2001, **222**, 427; (*c*) P. V. Kamat, *J. Phys. Chem. B*, 2002, **106**, 7729; (*d*) C. J. Murphy, T. K. Sau, A. M. Gole, C. J. Orendorff, J. Gao, L. Gou, S. E. Hunyadi and T. Li, *J. Phys. Chem. B*, 2005, **109**, 13857; (*e*) T. A. Taton, C. A. Mirkin and R. L. Letsinger, *Science*, 2000, **289**, 1757; (*f*) R. Sardar, M. Funston Alison, P. Mulvaney and W. Murray Royce, *Langmuir*, 2009, **25**, 13840.

2 (*a*) J. Turkevich, P. C. Stevenson and J. Hillier, *Discuss. Faraday Soc.*, 1951, **11**, 55; (*b*) J. Turkevich, P. C. Stevenson and J. Hillier, *J. Phys. Chem.*, 1953, **57**, 670.

3 (*a*) N. Wangoo, K. K. Bhasin, R. Boro and C. R. Suri, *Anal. Chim. Acta*, 2008, **610**, 142; (*b*) D. T. Nguyen, D.-J. Kim, M. G. So and K.-S. Kim, *Adv. Powder Technol.*, 2010, **21**, 111; (*c*) M. A. Uppal, A. Kafizas, T. H. Lim and I. P. Parkin, *New J. Chem.*, 2010, **34**, 1401.

4 Strong reducing reagent like: $NaBH_4$ (*a*) P. Lignier, M. Comotti, F. Schueth, J.-L. Rousset and V. Caps, *Catal. Today*, 2009, **141**, 355; borane (*b*) M. N. Martin, J. I. Basham, P. Chando and S.-K. Eah, *Langmuir*, 2010, **26**, 741; Stabilizing agents: thiols (*c*) M. J. Hostetler, J. E. Wingate, C.-J. Zhong, J. E. Harris, R. W. Vachet, M. R. Clark, J. D. Londono, S. J. Green, J. J. Stokes, G. D. Wignall, G. L. Glish, M. D. Porter, N. D. Evans and R. W. Murray, *Langmuir*, 1998, **14**, 17; tetroctylammonium bromide (*d*) M. Brust, M. Walker, D. Bethell, D. J. Schiffrin and R. Whyman, *J. Chem. Soc., Chem. Commun.*, 1994, 801; Polymer stabilizers: polyvinyl alcohol (PVA) (*e*) H. Shi, N. Xu, D. Zhao and B.-Q. Xu, *Catal. Commun.*, 2008, **9**, 1949; poly(*N*-vinyl-2-pyrrolidone) (PVP) (*f*) A. N. Grace and K. Pandian, *Colloids Surf., A*, 2006, **290**, 138; dendrimers (*g*) W. Vogel, D. G. Duff and A. Baiker, *Langmuir*, 1995, **11**, 401; Combined reagents: tetrakis(hydroxymethyl) phosphonium (*h*) W. W. Weare, S. M. Reed, M. G. Warner and J. E. Hutchison, *J. Am. Chem. Soc.*, 2000, **122**, 12890; triphenylphosphine (*i*) Y.-G. Kim, S.-K. Oh and R. M. Crooks, *Chem. Mater.*, 2004, **16**, 167.

5 (*a*) S. Marre and K. F. Jensen, *Chem. Soc. Rev.*, 2010, **39**, 1183; (*b*) S. Marre, J. Baek, J. Park, M. G. Bawendi and K. F. Jensen, *Jala*, 2009, **14**, 367; (*c*) T. Schwalbe, V. Autze, M. Hohmann and W. Stirner, *Org. Process Res. Dev.*, 2004, **8**, 440; (*d*) J. Baldyga and R. Pohorecki, *Chem. Eng. J.*, 1995, **58**, 183; (*e*) A. R. Bogdan, B. P. Mason, K. T. Sylvester and D. T. McQuade, *Angew. Chem., Int. Ed.*, 2007, **46**, 1698; (*f*) M. Pumera, *Chem. Commun.*, 2011, **47**, 5671.

6 (*a*) J. Wagner, T. Kirner, G. Mayer, J. Albert and J. M. Kohler, *Chem. Eng. J.*, 2004, **101**, 251; (*b*) J. M. Koehler, L. Abahmane, J. Wagner, J. Albert and G. Mayer, *Chem. Eng. Sci.*, 2008, **63**, 5048; (*c*) H. Tsunoyama, N. Ichikuni and T. Tsukuda, *Langmuir*, 2008, **24**, 11327; (*d*) S.-Y. Yang, F.-Y. Cheng, C.-S. Yeh and G.-B. Lee, *Microfluid. Nanofluid.*, 2010, **8**, 303; (*e*) J. Polte, R. Kraehnert, M. Radtke, U. Reinholz, H. Riesemeier, A. F. Thuenemann and F. Emmerling, *J. Phys.: Conf. Ser.*, 2010, **247**, 012051.

7 A. Gholamipour-Shirazi and C. Rolando, *Org. Process Res. Dev.*, 2012, **16**, 811.

8 (*a*) C. Li, D. Li, G. Wan, J. Xu and W. Hou, *Nanoscale Res. Lett.*, 2011, **6**, 440; (*b*) T. Muangnapoh, N. Sano, S.-I. Yusa, N. Viriya-empikul and T. Charinpanitkul, *Curr. Appl. Phys.*, 2010, **10**, 708; (*c*) G. Frens, *Nature, Phys. Sci.*, 1973, **241**, 20; (*d*) P. Zijlstra, C. Bullen, J. W. M. Chon and M. Gu, *J. Phys. Chem. B*, 2006, **110**, 19315; (*e*) X. Ji, X. Song, J. Li, Y. Bai, W. Yang and X. Peng, *J. Am. Chem. Soc.*, 2007, **129**, 13939; (*f*) I. Ojea-Jiménez, F. M. Romero, N. G. Bastus and V. Puntes, *J. Phys. Chem. C*, 2010, **114**, 1800.

9 (*a*) I. Ojea-Jimenez, N. G. Bastus and V. Puntes, *J. Phys. Chem. C*, 2011, **115**, 15752; (*b*) S. K. Sivaraman, S. Kumar and V. Santhanam, *J. Colloid Interface Sci.*, 2011, **361**, 543; (*c*) A. B. Smetana, J. S. Wang, J. Boeckl, G. J. Brown and C. M. Wai, *Langmuir*, 2007, **23**, 10429.

10 M. C. Fournier, L. Falk and J. Villermaux, *Chem. Eng. Sci.*, 1996, **51**, 5053.

11 (*a*) J. Kimling, M. Maier, B. Okenve, V. Kotaidis, H. Ballot and A. Plech, *J. Phys. Chem. B*, 2006, **110**, 15700; (*b*) G. Schmid, *Chem. Soc. Rev.*, 2008, **37**, 1909; (*c*) M. A. Watzky, E. E. Finney and R. G. Finke, *J. Am. Chem. Soc.*, 2008, **130**, 11959.

12 (*a*) J. Park, J. Joo, S. G. Kwon, Y. Jang and T. Hyeon, *Angew. Chem., Int. Ed.*, 2007, **46**, 4630; (*b*) V. Privman, D. V. Goia, J. Park and E. Matijevic, *J. Colloid Interface Sci.*, 1999, **213**, 36.

13 (*a*) S. Basu, S. K. Ghosh, S. Kundu, S. Panigrahi, S. Praharaj, S. Pande, S. Jana and T. Pal, *J. Colloid Interface Sci.*, 2007, **313**, 724; (*b*) P. A. Buining, B. M. Humbel, A. P. Philipse and A. J. Verkleij, *Langmuir*, 1997, **13**, 3921; (*c*) M. M. Alvarez, J. T. Khoury, T. G. Schaaff, M. N. Shafigullin, I. Vezmar and R. L. Whetten, *J. Phys. Chem. B*, 1997, **101**, 3706; (*d*) D. G. Duff, A. Baiker and P. P. Edwards, *Langmuir*, 1993, **9**, 2301.

14 B. N. Khlebtsov and N. G. Khlebtsov, *Colloid J.*, 2011, **73**, 118.

15 C. Y. Tsai, D. S. Lee, Y. H. Tsai, B. Chan, T. Y. Luh, P. J. Chen and P. H. Chen, *Mater. Lett.*, 2004, **58**, 2023.

